Reliability-Constrained Statistical Analysis of NASA CNEOS Fireball Events: Implications for Bolide Population Studies

Shreyas Khobragade

Vidyalankar Institute of Technology
Mumbai, Maharashtra, India

Corresponding Author:
shreyaskhobragade1002@gmail.com

ORCID:
0009-0008-8659-2970

An abstract based on this work has been accepted for presentation at the International Seminar on Aerospace Science and Technology (ISAST 2026).

July 24, 2026

Reliability-Constrained Statistical Analysis of NASA CNEOS Fireball Events: Implications for Bolide Population Studies

Shreyas Khobragade

Vidyalankar Institute of Technology, Mumbai, India
ORCID: 0009-0008-8659-2970

***Abstract*—The NASA Center for Near-Earth Object Studies (CNEOS) Fireball Database is one of the most widely used resources for investigating global bolide populations. However, variations in event reliability, detection thresholds, and observational coverage introduce potential selection biases that may influence inferred population statistics. While the database has been extensively employed in studies of meteoroid fluxes, atmospheric entry processes, and planetary defense, the quantitative impact of reliability-based filtering on large-scale fireball statistics remains insufficiently characterized.**

In this study, we analyze 1,064 fireball events recorded in the NASA CNEOS Fireball Database to quantify the influence of observational selection effects on inferred bolide population properties. The catalogue was partitioned into six subsets based on observation period, impact-energy thresholds, and reliability-related criteria, including full, post-2017, high-energy (> 0.45 kt), reliable, combined-reliable, and low-reliability populations. Statistical analyses included power-law fitting of impact-energy distributions, temporal trend estimation, area-normalized spatial distribution assessment, correlation analysis of impact energy and peak-brightness altitude, and non-parametric distribution comparison using Kolmogorov–Smirnov and Mann–Whitney U tests.

Results demonstrate persistent heavy-tailed scaling behaviour across multiple independently filtered populations. The full dataset, high-energy subset, and combined-reliable subset converge toward a consistent power-law exponent of approximately $\alpha \approx 1.94$, suggesting robust underlying population characteristics despite substantial differences in event selection. In contrast, the low-reliability subset yields a significantly steeper exponent ($\alpha \approx 2.55$), indicating that unreliable detections can substantially bias inferred scaling relationships. Distribution comparison tests reveal highly significant differences between reliability-constrained populations (KS p-values ranging from 10^{-34} to 10^{-119}; MWU p-values ranging from 10^{-23} to 10^{-78}). Spatial analyses indicate broadly uniform global distributions after area normalization, while high-energy events exhibit a weak negative relationship between impact energy and peak-brightness altitude (Spearman $\rho \approx -0.25$).

These findings quantify the magnitude of reliability-selection bias within the CNEOS Fireball Database and demonstrate that reliability-aware filtering is essential for obtaining consistent estimates of bolide population statistics. The stability of $\alpha \approx 1.94$ across multiple independently filtered populations suggests a robust underlying scaling behaviour, while deviations observed in low-reliability events highlight the importance of dataset quality in meteoroid population modelling. The methodology presented here provides a reproducible framework for evaluating observational biases in heterogeneous fireball catalogues and supports improved future studies of meteoroid fluxes, atmospheric entry processes, and planetary defense applications.

***Index Terms*—Fireballs, Bolides, NASA CNEOS Fireball Database, Meteoroid Population Statistics, Power-Law Scaling, Observational Bias, Reliability Filtering, Atmospheric Entry, Planetary Defense, Statistical Analysis**

I. Introduction

Bolides and fireballs represent some of the most energetic manifestations of meteoroid entry into the Earth's atmosphere [1]. These events provide valuable information about the size-frequency distribution, physical properties, and flux of near-Earth meteoroids, while also contributing to planetary defense efforts aimed at characterizing impact hazards [1][2]. Large fireball events have attracted increasing scientific attention because they serve as natural laboratories for investigating atmospheric entry processes, fragmentation mechanisms, energy deposition, and the broader population characteristics of small Solar System bodies [3][4].

The increasing availability of global observational datasets has significantly expanded opportunities for statistical investigations of bolide populations. Among these resources, the NASA Center for Near-Earth Object Studies (CNEOS) Fireball Database has become one of the most widely utilized catalogues for studying fireball activity on a global scale [5][6]. The database contains observations of atmospheric impact events recorded primarily by U.S. Government sensor systems and provides estimates of key physical parameters, including impact energy, altitude of peak brightness, velocity, and geographic location [5][6]. Due to its global coverage and long temporal record, the CNEOS database has been widely employed in studies of meteoroid fluxes, atmospheric entry phenomena, impact hazard assessment, and planetary defense applications [5][6][7].

Despite its extensive use, the CNEOS Fireball Database is not a homogeneous observational dataset [8]. Detection capabilities have evolved over time as sensor systems, processing methodologies, and reporting practices have changed [8]. Furthermore, event completeness varies as a function of impact energy, observational geometry, and measurement reliability [8]. Recent studies have highlighted the importance of considering these factors when interpreting population-level statistics derived from fireball catalogues [8]. In particular, reliability classifications and energy thresholds have been shown to influence the accuracy and consistency of derived physical parameters, suggesting that unfiltered analyses may be susceptible to observational selection effects [8].

While previous investigations have examined fireball occurrence rates, impact-energy distributions, and observational uncertainties, the quantitative influence of reliability-based filtering on large-scale bolide population statistics remains insufficiently characterized [2][9]. In particular, it remains unclear whether commonly reported statistical properties, such as power-law scaling behaviour, spatial distributions, and energy–altitude relationships, remain stable when the dataset is partitioned according to reliability-related criteria [2][9]. Establishing the robustness of these properties is important because many scientific and operational applications rely on statistical inferences derived from heterogeneous observational catalogues.

The objective of this study is to quantify the impact of observational selection effects and reliability-related filtering on inferred fireball population characteristics within the NASA CNEOS Fireball Database. To achieve this, the complete catalogue was partitioned into six subsets representing different levels of observational quality, temporal coverage, and impact-energy thresholds. Statistical analyses were then performed to evaluate impact-energy scaling behaviour, spatial distributions, temporal trends, and energy–altitude relationships across these populations. Additionally, non-parametric statistical tests were used to determine whether reliability-constrained subsets exhibit significantly different energy distributions.

By systematically comparing independently filtered populations, this work provides a reproducible framework for assessing observational bias within heterogeneous fireball catalogues. The resulting analysis contributes to ongoing efforts aimed at improving meteoroid population modelling, atmospheric-entry studies, and planetary defense applications through more robust interpretation of global fireball observations.

II. Dataset Description

A. NASA CNEOS Fireball Database

The dataset used in this study was obtained from the NASA Center for Near-Earth Object Studies (CNEOS) Fireball Database, a publicly accessible catalogue of globally detected fireball and bolide events [5]. The database contains observations derived primarily from U.S. Government sensor systems and provides information on the physical and observational characteristics of atmospheric impact events [5]. Reported parameters include event date and time, geographic coordinates, peak brightness altitude, velocity, total radiated energy, and estimated impact energy [6].

The CNEOS Fireball Database is widely used in studies of meteoroid populations, atmospheric entry processes, impact hazard assessment, and planetary defense applications because of its extensive temporal coverage and global observational scope [5]. However, the heterogeneous nature of the observations introduces potential biases related to detection sensitivity, observational coverage, and event reliability, making the database an appropriate case study for evaluating the influence of selection effects on inferred population statistics [8].

B. Dataset Preparation

A total of 1,064 fireball events available at the time of analysis were extracted from the database. Geographic coordinates reported in degree-direction format were converted into numerical latitude and longitude values to facilitate spatial analyses and global visualization. Event timestamps were converted into standard datetime representations, allowing extraction of temporal information such as observation year and month.

Events with missing values were retained whenever possible to preserve sample size for analyses that did not require the missing parameter. For spatial analyses, only events containing valid geographic coordinates were included. Consequently, 878 events were available for global mapping and spatial-density calculations, while the remaining events lacked sufficient location information for geographic analysis.

C. Reliability-Constrained Subsets

To investigate the effects of observational selection and event reliability, the complete dataset was partitioned into six subsets representing different filtering strategies and data-quality conditions.

- **The Full Dataset** ($n = 1,064$) served as the reference population and included all available events.
- **The Post-2017 Dataset** ($n = 311$) contained events recorded from 2017 onward, representing a period associated with improved observational consistency and increased reporting completeness [8][10].
- **The High-Energy Dataset** ($n = 241$) included events with estimated impact energies greater than 0.45 kilotons TNT equivalent. This threshold was selected to reduce the influence of low-energy detection incompleteness and to focus on events more consistently observed by the underlying sensor network [8][10].
- **The Reliable Dataset** ($n = 57$) consisted of events satisfying the strictest reliability-related metadata criteria available within the CNEOS catalogue, including quality indicators associated with improved measurement confidence.
- **The Combined-Reliable Dataset** ($n = 495$) included events satisfying one or more reliability-related metadata conditions and represents an intermediate-quality population between the strict reliability subset and the complete catalogue.
- **The Low-Reliability Dataset** ($n = 569$) comprised events that did not satisfy the selected reliability constraints and was used to evaluate the influence of potentially uncertain detections on population-level statistics.

These subsets enable direct assessment of how observational quality, detection thresholds, and temporal coverage influence inferred properties of the global fireball population.

III. Methodology

A. Data Preprocessing

All analyses were performed using Python-based scientific computing libraries, including `Pandas`, `NumPy`, `SciPy`, `Scikit-Learn`, and the `Powerlaw` package.

Geographic coordinates reported within the NASA CNEOS Fireball Database were converted from degree-direction notation (e.g., 45.2°N, 120.5°W) into signed numerical latitude and longitude values. Event timestamps were transformed into standard datetime objects, enabling extraction of observation year and month information for temporal analyses.

Records containing missing values were retained whenever possible and excluded only from analyses requiring the unavailable parameter. This approach maximized sample utilization while preserving statistical consistency across different investigations.

B. Power-Law Analysis of Impact Energy

To evaluate the scaling behaviour of bolide impact energies, power-law distributions were fitted to the calculated total impact energy values reported in kilotons (kt) TNT equivalent [2][11].

Only events with impact energies exceeding 0.1 kt were considered during fitting to reduce the influence of incomplete low-energy detections and measurement uncertainty [8][9]. Power-law parameters were estimated using maximum-likelihood methods implemented in the `Powerlaw` package [11]. For each dataset, the scaling exponent (α), lower cutoff value ($x_{\min}$), and Kolmogorov–Smirnov goodness-of-fit statistic were calculated.

To assess whether a power-law model provided a reasonable description of the observed distributions, log-likelihood ratio comparisons between power-law and lognormal alternatives were additionally computed [11].

C. Energy–Altitude Correlation Analysis

The relationship between impact energy and peak-brightness altitude was investigated using both Pearson and Spearman correlation coefficients [2].

Pearson correlation was used to quantify linear relationships between impact energy and altitude, while Spearman rank correlation was employed to evaluate monotonic relationships that may not be strictly linear. Statistical analyses were performed only on events containing valid measurements for both variables.

Because bolide energy distributions are strongly skewed and may violate normality assumptions, Spearman correlation was considered the primary indicator of association.

D. Temporal Trend Analysis

Long-term temporal behaviour was examined by aggregating fireball detections by calendar year.

Annual event counts were calculated for each dataset and fitted using ordinary least-squares linear regression. The resulting regression slope was used to quantify increasing or decreasing trends in observed detection frequency, while the coefficient of determination (R^2) was used to evaluate the strength of the fitted relationship.

Events recorded during 2026 were excluded from temporal trend calculations because the year was incomplete at the time of analysis and could introduce artificial bias into annual count estimates.

E. Spatial Distribution Analysis

Spatial distributions were examined using geographic coordinates and latitude-band density calculations [9].

The Earth's surface was divided into six latitude zones spanning 30-degree intervals between $-90°$ and $+90°$. Event counts within each latitude band were normalized by the corresponding spherical surface area represented by that latitude range. This normalization accounts for the decreasing surface area of latitude bands toward the poles and enables direct comparison of event densities across geographic regions.

For each dataset, the mean spatial density, standard deviation, and coefficient of variation (CV) were calculated. Lower CV values indicate greater spatial uniformity, whereas larger values suggest stronger geographic clustering or observational bias.

F. Distribution Comparison Tests

To quantify the influence of selection criteria on inferred impact-energy populations, pairwise statistical comparisons were performed between key dataset subsets.

The two-sample Kolmogorov–Smirnov (KS) test was used to determine whether two energy distributions originated from the same underlying population. The KS statistic measures the maximum separation between cumulative distribution functions, while the associated p-value evaluates statistical significance.

Because impact-energy distributions are highly non-normal, the Mann–Whitney U (MWU) test was additionally applied as a non-parametric alternative for comparing population distributions. The MWU test evaluates whether one population tends to contain systematically larger values than another without assuming any specific underlying distribution.

Comparisons were conducted between the Reliable and Low-Reliability subsets, Full and Reliable subsets, Full and High-Energy subsets, and Combined-Reliable and Low-Reliability subsets. These tests provide a quantitative assessment of how reliability filtering and energy thresholds influence inferred bolide population characteristics.

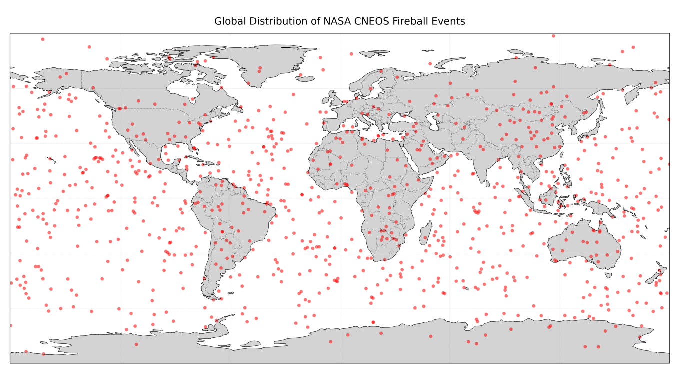

Fig. 1. Global distribution of fireball events recorded in the NASA CNEOS database. A total of 878 events with valid geographic coordinates were included in the spatial analysis.

IV. Results

A. Global Spatial Distribution of Fireball Events

Fig. 1 illustrates the global distribution of 1,064 fireball events recorded in the NASA CNEOS Fireball Database. Events are observed across all major geographic regions and oceanic areas, reflecting the near-global observational coverage of satellite-based fireball detection systems. No obvious large-scale clustering is apparent, suggesting that observed fireball occurrences are broadly distributed worldwide.

To assess potential geographic sampling biases, event frequencies were normalized by the surface area represented by individual latitude bands, as shown in Fig. 5. Area-normalized densities remained relatively consistent across most latitude intervals, indicating that the observed distribution is broadly compatible with spatial uniformity. High-energy and reliability-constrained subsets exhibited similar behaviour, although modest variations were observed at higher latitudes where event counts are comparatively smaller. These findings are consistent with previous statistical investigations of global fireball occurrence patterns [9]. Spatial density coefficients of variation ranged from 0.0746 to 0.2260 across analyzed subsets, supporting the interpretation that large-scale geographic biases are limited within the dataset.

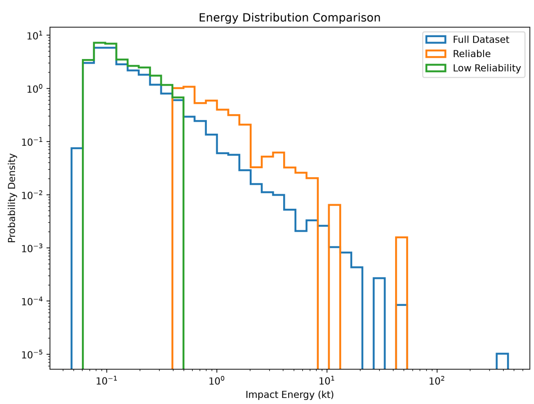

Fig. 2. Impact-energy probability density distributions for the full, reliable, and low-reliability datasets, illustrating differences in energy characteristics across reliability-constrained populations.

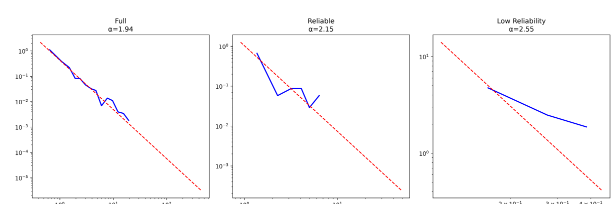

Fig. 3. Power-law fits to the impact-energy distributions of the full, reliable, and low-reliability datasets. Dashed lines indicate fitted power-law models.

B. Impact-Energy Distribution Characteristics

The impact-energy distributions of the full dataset and reliability-constrained subsets are shown in Fig. 2. All populations exhibit strongly right-skewed distributions characteristic of heavy-tailed natural phenomena, with a large number of low-energy events and progressively fewer high-energy impacts.

The reliable subset displays a greater proportion of higher-energy events than the low-reliability population, reflected by its substantially larger lower-bound energy threshold ($x_{\min} = 0.91$ kt compared with the low-reliability subset 0.11 kt). Conversely, the low-reliability subset is dominated by lower-energy detections, indicating greater sensitivity to measurement uncertainty near observational thresholds.

C. Power-Law Scaling Behaviour

Power-law fits to the impact-energy distributions are presented in Fig. 3. The full dataset yielded a scaling exponent of $\alpha = 1.9392$ above a minimum energy threshold of 0.43 kt. Nearly identical exponents were obtained for both the high-energy subset ($\alpha = 1.9366$) and the combined-reliable subset ($\alpha = 1.9366$), indicating remarkable consistency across independently filtered populations despite differences in event-selection criteria.

The post-2017 subset produced a comparable exponent of $\alpha = 1.9677$, suggesting that improvements in observational capabilities after 2017 did not substantially alter the inferred scaling behaviour of the observed fireball population. In contrast, the low-reliability subset exhibited a substantially steeper exponent ($\alpha = 2.5486$), while the strictly reliable subset produced $\alpha = 2.1473$.

A summary of scaling exponents is provided in Fig. 4. The convergence of multiple subsets toward $\alpha \approx 1.94$ suggests the presence of a robust underlying heavy-tailed distribution, whereas departures observed in lower-quality subsets indicate sensitivity to observational uncertainty and selection effects, consistent with previously reported heavy-tailed energy-frequency relationships for bolide populations [2].

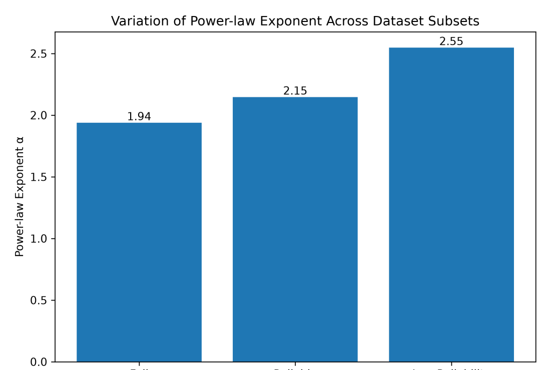

Fig. 4. Comparison of fitted power-law exponents (α) across dataset subsets, illustrating the influence of filtering criteria on inferred scaling behaviour.

D. Statistical Separation Between Reliability-Constrained Populations

To evaluate whether reliability-based filtering produces statistically distinct populations, pairwise comparisons were performed using Kolmogorov–Smirnov (KS) and Mann–Whitney U (MWU) tests. The resulting significance levels are summarized in Fig. 6.

TABLE I
SUMMARY STATISTICS FOR RELIABILITY-CONSTRAINED SUBSETS OF THE NASA CNEOS FIREBALL DATABASE.

Dataset	N	α	$x_{\min}$ (kt)	Spearman ρ	Trend Slope	R^2	Spatial CV
Full Dataset	1064	1.939	0.43	-0.118	0.829	0.496	0.164
Post-2017	311	1.968	0.11	-0.142	-1.238	0.441	0.226
High-Energy	241	1.937	0.46	-0.254	0.105	0.115	0.075
Combined-Reliable	495	1.937	0.46	-0.169	0.961	0.581	0.162
Reliable	57	2.147	0.91	-0.087	-0.595	0.191	0.214
Low-Reliability	569	2.549	0.11	0.003	0.645	0.285	0.178

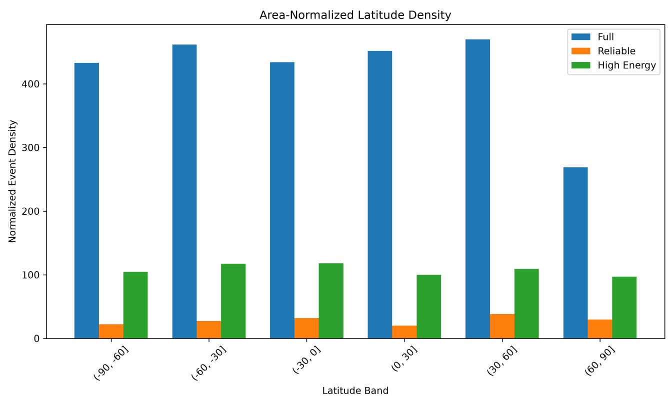

Fig. 5. Area-normalized latitude-band event densities for the full, reliable, and high-energy datasets used to assess large-scale spatial distribution patterns.

The strongest separation was observed between reliable and low-reliability populations (KS $p = 4.43 \times 10^{-82}$; MWU $p = 1.21 \times 10^{-35}$), demonstrating that the two subsets originate from markedly different energy distributions. Similar results were obtained for comparisons between the full and reliable populations (KS $p = 4.24 \times 10^{-34}$; MWU $p = 1.34 \times 10^{-23}$), the full and high-energy populations (KS $p = 2.69 \times 10^{-119}$; MWU $p = 1.20 \times 10^{-78}$), and the combined-reliable and low-reliability populations (KS $p = 3.72 \times 10^{-58}$; MWU $p = 2.37 \times 10^{-30}$).

These results provide strong statistical evidence that reliability-related filtering substantially alters the composition of observed fireball populations and therefore influences derived population-level characteristics. This finding supports recent studies demonstrating that measurement quality and observational constraints can affect the reliability of parameters derived from the CNEOS database [8], [10].

E. Energy–Altitude Relationships and Temporal Trends

Spearman rank correlation analysis revealed generally weak negative relationships between impact energy and peak-brightness altitude. The strongest correlation occurred within the high-energy subset ($\rho = -0.2538$), although the magnitude of the relationship remained weak, suggesting that larger events tend to reach peak luminosity at slightly lower atmospheric altitudes.

Temporal trend analysis produced mixed results across subsets. The full dataset and combined-reliable populations exhibited positive trend slopes of 0.8294 and 0.9608, respectively, while the post-2017 subset showed a negative trend slope (-1.2381). However, coefficients of determination remained moderate ($R^2 = 0.11$–0.58), indicating that temporal variability is likely influenced by observational and selection-related effects in addition to any underlying physical trends.

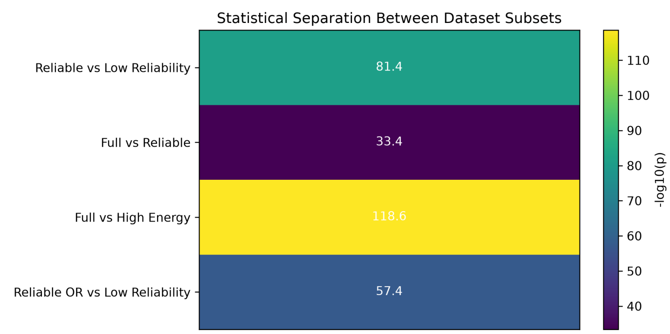

Fig. 6. Statistical separation between dataset subsets quantified using Kolmogorov–Smirnov and Mann–Whitney U tests. Values are expressed as $-\log_{10}(p)$, with larger values indicating stronger statistical separation.

TABLE II
PAIRWISE STATISTICAL COMPARISONS BETWEEN RELIABILITY-CONSTRAINED POPULATIONS USING KOLMOGOROV–SMIRNOV (KS) AND MANN–WHITNEY U (MWU) TESTS.

Comparison	KS p	MWU p
Reliable vs Low Reliability	4.43×10^{-82}	1.21×10^{-35}
Full vs Reliable	4.24×10^{-34}	1.34×10^{-23}
Full vs High Energy	2.69×10^{-119}	1.20×10^{-78}
Combined-Reliable vs Low Reliability	3.72×10^{-58}	2.37×10^{-30}

V. DISCUSSION

A. Robustness of Energy Scaling Behaviour

The most significant outcome of this study is the remarkable stability of the impact-energy scaling exponent across multiple independently filtered populations. Despite substantial differences in event-selection criteria, the full dataset, high-energy subset, and combined-reliable population consistently produced power-law exponents near $\alpha \approx 1.94$. This persistence suggests that the observed heavy-tailed energy distribution reflects an intrinsic characteristic of the recorded fireball population rather than an artifact introduced by a particular filtering strategy. The exponent obtained here is broadly consistent with previous bolide population studies based on satellite observations [2].

The consistency of these independently derived exponents implies that moderate variations in observational coverage, energy thresholds, and reliability constraints do not substantially alter the dominant statistical behaviour of the dataset.

Consequently, the value $\alpha \approx 1.94$ may provide a useful reference estimate for future population-level studies utilizing the NASA CNEOS Fireball Database.

B. Reliability-Selection Effects and Population Inference

While several subsets converged toward similar scaling behaviour, the low-reliability population exhibited a substantially steeper exponent ($\alpha \approx 2.55$). This divergence indicates that reliability-related selection effects can significantly influence inferred population statistics. The strong statistical separation observed between reliability-constrained populations further supports the interpretation that low-reliability events represent a distinct observational regime rather than simple random variations within the broader dataset.

These findings suggest that reliability filtering should not be viewed solely as a data-cleaning procedure. Recent investigations have similarly emphasized that observational quality and measurement uncertainty can influence the reliability of parameters derived from CNEOS fireball observations [8]. Instead, reliability metrics directly influence estimates of population scaling relationships and may affect derived quantities such as impact frequencies and energy distributions. Analyses that ignore reliability-related information risk introducing systematic biases into population-level inference.

C. Spatial and Temporal Characteristics

Area-normalized spatial analyses indicate that the global distribution of recorded fireball events is broadly uniform after accounting for geographic area [9]. The absence of strong persistent clustering is consistent with expectations for impactors arriving from a wide range of heliocentric trajectories and supports the assumption of approximate large-scale geographic homogeneity within the observed population.

Temporal analyses produced more variable behaviour across subsets. Given the known evolution of observational capabilities and reporting practices throughout the observational period, these trends are likely influenced by changing detection characteristics in addition to any underlying physical variability [8]. Consequently, temporal patterns should be interpreted cautiously when using heterogeneous observational catalogues [8].

D. Energy–Altitude Relationships

A weak negative relationship between impact energy and peak-brightness altitude was observed within the high-energy population. Although modest in magnitude, this trend is physically plausible because larger and more energetic bolides can penetrate deeper into the atmosphere before releasing a significant fraction of their energy. However, the weak correlation indicates that atmospheric entry behaviour cannot be explained by impact energy alone and is likely influenced by additional parameters such as entry velocity, composition, fragmentation processes, and entry geometry [1], [4].

E. Implications for Bolide Population Studies

The primary contribution of this work is the quantitative assessment of reliability-selection bias within one of the most widely used global fireball catalogues. The results demonstrate that while the overall scaling behaviour of the CNEOS dataset remains remarkably stable under several independent filtering strategies, low-reliability events can significantly alter inferred population characteristics.

These findings have implications for meteoroid flux estimation, atmospheric entry modelling, and planetary defense applications, all of which rely upon accurate characterization of impact-energy distributions. More broadly, the reliability-constrained framework developed here provides a reproducible approach for evaluating observational biases in heterogeneous astronomical catalogues and may be extended to future fireball and small-body population studies [1], [2], [4], [8].

VI. Conclusion

This study presents a reliability-constrained statistical analysis of 1,064 fireball events from the NASA CNEOS Fireball Database to evaluate the influence of observational selection effects on inferred bolide population properties. By partitioning the catalogue into six subsets based on observation period, impact-energy threshold, and reliability-related criteria, we systematically assessed the stability of commonly reported fireball statistics under different filtering conditions.

Power-law analyses revealed that the full dataset, high-energy subset, and combined-reliable subset consistently yielded scaling exponents near $\alpha \approx 1.94$, indicating a robust underlying heavy-tailed energy distribution despite substantial differences in event selection. In contrast, the low-reliability population produced a significantly steeper exponent ($\alpha \approx 2.55$), demonstrating that unreliable detections can substantially alter inferred population characteristics. Non-parametric distribution comparison tests further confirmed statistically significant differences between reliability-constrained subsets, highlighting the measurable impact of data-quality considerations on population-level analyses.

Spatial analyses showed broadly uniform global distributions after area normalization, while correlation analyses identified a weak negative relationship between impact energy and peak-brightness altitude for high-energy events. Temporal analyses suggested that observed detection trends are influenced by both observational completeness and evolving sensor capabilities, emphasizing the importance of considering catalogue heterogeneity when interpreting long-term fireball statistics.

Overall, the results demonstrate that reliability-aware filtering is essential for obtaining consistent and reproducible estimates of bolide population properties from heterogeneous observational databases. The persistence of a common scaling exponent across multiple independently filtered populations suggests that robust statistical characteristics can be recovered despite observational limitations, provided that appropriate quality controls are applied.

Future work may extend this framework through integration with ground-based fireball networks, infrasound observations, and additional meteoroid catalogues to further investigate detection biases, improve population modelling, and support planetary defense and atmospheric-entry studies. The methodology developed here provides a reproducible foundation for evaluating observational uncertainty in large-scale fireball datasets and may be applicable to other heterogeneous astronomical catalogues.

ACKNOWLEDGMENTS

AI-assisted tools were used for language refinement, manuscript editing, and literature discovery. All analyses, interpretations, and conclusions were independently verified by the author.

REFERENCES

[1] Z. Ceplecha, J. Borovička, W. G. Elford, D. O. ReVelle, R. L. Hawkes, V. Porubčan, and M. Šimek, "Meteor phenomena and bodies," *Space Science Reviews*, vol. 84, no. 3, pp. 327–471, 1998.

[2] P. Brown, R. Spalding, D. O. ReVelle, E. Tagliaferri, and S. Worden, "The flux of small near-earth objects colliding with the earth," *Nature*, vol. 420, no. 6913, pp. 294–296, 2002.

[3] P. G. Brown, J. D. Assink, L. Astiz, R. Blaauw, M. B. Boslough, J. Borovička, N. Brachet, D. Brown, M. Campbell-Brown, L. Ceranna *et al.*, "A 500-kiloton airburst over chelyabinsk and an enhanced hazard from small impactors," *Nature*, vol. 503, no. 7475, pp. 238–241, 2013.

[4] J. G. Hills and M. P. Goda, "The fragmentation of small asteroids in the atmosphere," *Astronomical Journal (ISSN 0004-6256), vol. 105, no. 3, p. 1114-1144.*, vol. 105, pp. 1114–1144, 1993.

[5] NASA/JPL Center for NEO Studies, "Fireball and bolide data," https://cneos.jpl.nasa.gov/fireballs/, 2026, accessed: 2026-06-21.

[6] E. A. Silber and V. Sawal, "Blade: An automated framework for classifying light curves from the center for near-earth object studies fireball database," *The Astronomical Journal*, vol. 170, no. 3, p. 153, 2025.

[7] E. Peña-Asensio, J. M. Trigo-Rodríguez, and A. Rimola, "Orbital characterization of superbolides observed from space: dynamical association with near-earth objects, meteoroid streams, and identification of hyperbolic meteoroids," *The Astronomical Journal*, vol. 164, no. 3, p. 76, 2022.

[8] E. Peña-Asensio, H. Socas-Navarro, and D. Z. Seligman, "Error dependencies in the space-based cneos fireball database," *Astronomy & Astrophysics*, vol. 701, p. A202, 2025.

[9] A. S. Betzler, "Statistical and probabilistic analysis of meteor and superbolide observations from ground and space platforms," *Monthly Notices of the Royal Astronomical Society*, vol. 540, no. 1, pp. 60–70, 2025.

[10] M. Hajdukova, G. Stober, D. Barghini, P. Koten, J. Vaubaillon, V. J. Sterken, S. Ďurišová, A. Jackson, and S. Desch, "No evidence for interstellar fireballs in the cneos database," *Astronomy & Astrophysics*, vol. 691, p. A8, 2024.

[11] A. Clauset, C. R. Shalizi, and M. E. Newman, "Power-law distributions in empirical data," *SIAM review*, vol. 51, no. 4, pp. 661–703, 2009.